Peer-reviewed version available at *Molecules* **2018**, *23*, 1893; doi:10.3390/molecules23081893

Article

Comprehensive Snake Venomics of the Okinawa Habu Pit Viper, *Protobothrops Flavoviridis*, by Complementary Mass Spectrometry-Guided Approaches

Maik Damm [1,†], Benjamin-Florian Hempel [1,†], Ayse Nalbantsoy [2] and Roderich D. Süssmuth [1,*]

[1] Department of Chemistry, Technische Universität Berlin, 10623 Berlin, Germany; maik.damm@tu-berlin.de (M.D.); benjamin.hempel@chem.tu-berlin.de (B.-F.H.)

[2] Department of Bioengineering, Ege University, 35100 Izmir, Turkey; analbantsoy@gmail.com (A.N.)

* Correspondence: roderich-suessmuth@tu-berlin.de; Tel.: +49-30-314-24205

† These authors contributed equal to this work

Abstract: The Asian world is home to a multitude of venomous and dangerous snakes, which are attributed to various medical effects used in the preparation of traditional snake tinctures and alcoholics, like the Japanese snake wine, named Habushu. The aim of this work was to perform the first quantitative proteomic analysis of the *Protobothrops flavoviridis* pit viper venom. Accordingly, the venom was analyzed by complimentary bottom-up and top-down mass spectrometry techniques. The mass spectrometry-based snake venomics approach revealed that more than half of the venom is composed of different phospholipases A2 (PLA_2). The combination with an intact mass profiling led to the identification of the three main Habu PLA_2s. Furthermore, nearly one-third of the total venom consists of snake venom metalloproteinases and disintegrins, and several minor represented toxins families were detected: CTL, CRISP, svSP, LAAO, PDE and 5'-nucleotidase. Finally, the venom of *P. flavoviridis* contains certain bradykinin-potentiating peptides and related peptides, like the svMP inhibitors pEKW, pEQW, pEEW and pENW. In preliminary MTT cytotoxicity assays the highest cancerous-cytotoxicity of the crude venom was measured against human neuroblastoma SH-SY5Y cells and shows in some fractions disintegrin-like effects.

Keywords: Snake venomics; Viperidae; *Protobothrops flavoviridis*; Habu pit viper; Bottom-Up; Top-Down; BPP; Tripeptide metalloprotease inhibitor; Cytotoxicity

1. Introduction

Since ancient times, people have been fascinated by snakes and ascribed them a diverse set of properties and character traits. Especially, in the mythology, from South America through ancient Egypt to the Asian world, snakes and snake-like creatures represent both, good and evil [1–4]. Most of them appear as symbols of wisdom and protection, whereby also healing aspects have often been attributed [4]. Even today, the Aesculapius, the snake-wrapped rod of the Hellenic god Asclepius, and the winged Caduceus of Hermes symbolize medical, as well as veterinarian's and pharmacist's professions [1]. On the other hand, based on encounters with humans, snakes are also known and feared for their bites and the possible consequences. The most accidents with snakes were registered in the tropics mainly of farmers by contact during the field work. In consequence, snake envenomation was resumed during 2017 to the list of neglected tropical diseases [5].

One of peril regions is Japan, home to more than 38 different venomous and non-venomous snakes [6]. They coexist with man over the entire country even on the smaller islands, wherein the diverse climatic conditions play a decisive role in the distribution of snakes [7]. The more densely inhabited areas exhibit a higher risk of bites and envenomation, which is further increased in the subtropical regions during the warm summer months [7]. Representatives of the most dangerous

Peer-reviewed version available at Molecules 2018, 23, 1893; doi:10.3390/molecules23081893

snake families in Japan are the Habu (*Protobothrops flavoviridis*; *P. flavoviridis*) and Mamushi (*Gloydius blomhoffii*) pit vipers, as well as the colubrid Yamakagashi (*Rhabdophis tigrinus*) and the oceanic Erabu Umi Hebi (*Laticauda semifasciata*) [7–9].

Particularly in several Asian but also in other countries, many mostly dangerous snakes were used in special traditionally medicines, e.g. in Japan the *P. flavoviridis*, also known as Okinawa Habu, which gave the Habushu snake wine its name by adding a snake or snake extract [10,11]. Commonly, these liquors contain high ethanol concentrations of ~40% and are unproblematic to consume, but in home-made liquors also lower ethanol concentrations are feasible, so that in rare cases drinking could cause intoxications but could lead from health impairment up to damages [12].

The Japanese Habu viper is a member of the venomous pit viper subfamily. In some cases, *P. flavoviridis* is classified to another genus and named *Trimeresurus flavoviridis* [13]. This snake is endemic to 25 islands between Japan and Taiwan, whereas the largest areas of distribution are the Amami (Kagoshima Prefecture) and the Okinawa Islands (Okinawa Prefecture). Morphological and genetic differences of these populations are still under study, whereby a genetic gap between two island populations were shown [14,15]. The Habu is responsible for the most envenomations on the Amami Ohshima islands and nearby regions [16]. A bite, like one of other vipers, could lead from less dangerous more local symptoms (pain, erythema, vomiting) to more dramatic symptoms, such as necrosis, acute kidney injury and death, so that at the beginning of the 20th century the mortality rate was at 10% [16,17]. The enhanced medical supply chains helped to decrease the mortality to nearly 1% until 2013 [16]. One further main reason for a lowered mortality is the development of potent antivenoms, which are until now the only effective treatment of snake envenomation [18]. Since the start of antivenom serotherapy trials against snake bites, more than 120 years have elapsed, but until today snakebites are still a serious threat to human particularly those working in endemic areas [5,19]. The composition of venoms defines the effect of an envenomation and is relevant for the development of specific and effective antivenoms but it also could provide components with physiological functions exploited for the development of drugs [20]. Hence, apart from the investigation of snake venoms for providing therapies and cures of snake bites, the exploration of the drug potential represents an important aspect of venom research.

As already mentioned above, venoms are a complex mixture of low molecular weight substances, e.g. nucleotides, sugars and lipids, as well as of different peptides and proteins the latter with enzymatic and non-enzymatic functions [21–24]. Habitat variation and the divergence of prey exerting an evolutionary pressure are major aspects that could lead to changes in the venom composition [15,25,26]. Even if the percentage composition could differ from species to species and also between different separated populations of the same species, the main toxin families in snakes have been mostly identified [23,27]. The toxins of vipers range from small natriuretic peptides and bradykinin-potentiating peptides (BPPs) over cysteine-rich secretory proteins (CRISPs) and phospholipases A2 (PLA_2s) to high molecular serine- and metalloproteinases (svSPs, svMPs) [25,28].

The venom of *P. flavoviridis* has been under investigation for decades and is still a source of new findings e.g. as in the case of C-type lectin-like proteins (CTL), which are known for their strong effect on platelet aggregation [29–34]. Hence, two CTLs were firstly identified from the Habu snake venom. One CTL binds the blood coagulation factors IX and X (named IX/X-BP), whereas the second has been described as an antagonist of the Willebrand factor receptor GPIb and called flavocetin-A [35,36]. Recent studies have shown that flavocetin-A as a long known protein also inhibits the collagen-binding $\alpha 2\beta 1$ integrin, which is the main receptor of platelets and necessary for platelet activation and cell activation [31,37].

Previous studies on the venom of *P. flavoviridis* were transcriptomic approaches and proteomic studies however limited to shot-gun analysis, which could not provide a detailed picture of the venome composition [29,38]. Here we report the first quantitative analysis of the *P. flavoviridis* venom by a combination of diverse mass spectrometric methods to give a more accurate profile of the venom and its composition. Therefore, a combined proteomic approach of bottom-up (BU) and top-down (TD) mass spectrometry (MS), including intact mass profiling (IMP), was used for snake venomic analyses, thus ensuring a high annotation coverage of the whole venom [39–41].

Peer-reviewed version available at Molecules 2018, 23, 1893; doi:10.3390/molecules23081893

2. Results

2.1. Top-down analysis

In a first top-down (TD) analytical run the venom of *P. flavoviridis* was analyzed by a venomic workflow to quickly identify the occurring native peptides and proteins. The application of the intact mass profiling (IMP) revealed 80 different molecular masses (Figure 1, Table S1). Proteins could be detected up to a size of ~31 kDa: 9 proteins in a range of 13-15 kDa and 6 in the range of 21-31 kDa. Dominant mass signals of small peptides at *m/z* 430-617 were observed at early gradient retention times in peaks 1-7. The small molecular determinants could be annotated manually and identified as members of the bradykinin-potentiating peptides related peptides (BPP-RP) (Figure S1-S9) [42,43]. The peaks 8-15 exhibited mainly masses of 7-8 kDa putatively identified as disintegrins (DI) by IMP and later confirmed by BU annotation. While the components with molecular masses of ~14 kDa including peaks 16, 17, 18 and 22 were identified as PLA2s, the molecular masses of 21-28 kDa were suspected members of the svSP and CTL family (Table S1).

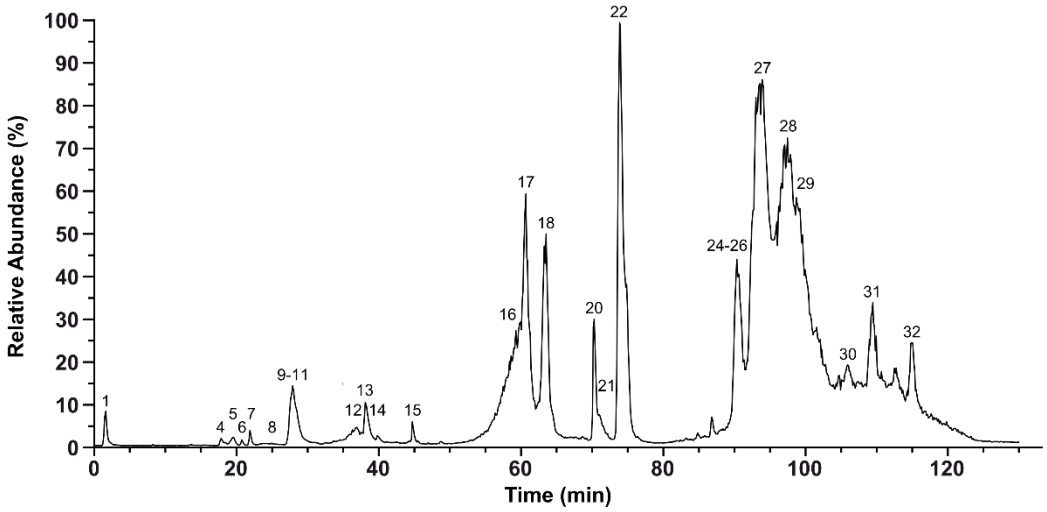

Figure 1. Total ion chromatogram of *P. flavoviridis* venom for IMP and TD. The total ion counts from *P. flavoviridis* crude venom were measured by HPLC-ESI-MS of native crude venom. The relative abundance was set to 100% for the highest peak. The peak nomenclature is based on the chromatogram fractions (shown in Figure 2) The identified molecular masses of intact peptides and proteins are listed Table S1.

Accordingly, the non-reduced venom of *P. flavoviridis* revealed 9 different proteins belonging to five toxin families: PLA2, svMP, DI, BPP-RP and L-amino acid oxidases (LAAO) (Table S1). Interestingly, most sequences were identified as fragments belonging to svMPs, which however were attributed to self-digestion e.g. by metalloproteinases, an effect described previously *in vitro* for bothropasin and brevilysin H6 [44].

Three different BPP-related peptides were annotated containing a characteristic pyro-glutamylated N-terminus (Table S1). Additionally, five protein masses were detected as full-length proteins. Each of these, a disintegrin as well as the four PLA2s, was annotated with different modifications (Table S1), since these mass differences to the expected amino acid sequence were indicated as a part of a longer fragment and not at a distinct position, we assume the identification of closely related isoforms.

In order to further increase the number of annotations and assignments achieved so far, a chemically reduced venom sample was measured (Figure S10). The reduction of cystines, which are important post-translational modifications (PTMs) in snake venoms, breaks up the tertiary structures and leads to a better fragmentation and *de novo* sequencing [40]. By means of the reduced TD approach, we detected, amongst other fragments, proteoforms of two 14 kDa toxins. One CTL with a

Peer-reviewed version available at Molecules 2018, 23, 1893; doi:10.3390/molecules23081893

monoisotopic molecular mass of 14400.38 Da was identified as a 31.11 Da lighter variant of the so called IX/X-BP CTL. The second mass (13921.36 Da) belongs to the PLA_2 family and was annotated as a proteoform of the basic phospholipase A_2 PL-X (13971.41 Da). The reductive workup of venom with TCEP ultimately leads to conformational changes of the proteins and thus to differences in retention time. Therefore, a peak assignment in comparison to the native TD TIC nomenclature was not possible.

Except for the BPP-RP, other isoforms of venom proteins were only detectable as fragments. It is worth mentioning, that of the 73 TD assignments of the reduced venom only three were annotated as internal fragments, while 54 belong to the N-terminal end and only 13 to the C-terminal end of the compared sequences. The *de novo* sequences were assigned to seven toxin families (Table 1). The high number of observed fragments could be an effect of the earlier mentioned digestion by metalloproteinases, and thus an accurate peak annotation in correlation with the native venom TD was impeded.

Table 1. Identified proteoforms and fragments of *P. flavoviridis* by reduced top-down analytics. Assignment of reduced crude venom component fragments by top-down (TD). Sequence tags were obtained *de novo* from MS/MS spectra and identified against a *P. flavoviridis* NCBI protein database (taxid: 88087) by TopPIC.

Toxin families	Protein ID	Highest E-value	NCBI Accession no.	No. of sequence proteoforms
PLA_2	basic phospholipase A_2 BP-III	8.21E-16	C7G1G6.1	20
	basic phospholipase A_2 PL-B	7.42E-15	P59265.1	11
	phospholipase A_2	7.85E-10	1202299A	11
	basic phospholipase A_2 PL-X	8.35E-10	P06860.1	5
	basic phospholipase A_2 PLA-A	2.98E-14	P59264.1	3
	basic phospholipase A_2 BP-II	3.70E-06	P0DJJ9.1	2
	basic phospholipase A_2 BP-I	8.90E-06	P0DJJ8.1	2
	phospholipase A_2	4.17E-03	BAA01561.1	2
	basic phospholipase A_2 PL-Y	2.37E-08	Q90Y77.1	1
svMP	zinc metalloproteinase/disintegrin	1.29E-06	P18619.2	3
	P-II metalloprotease	5.12E-05	BAN89360.1	1
	snake venom metalloproteinase HR2a	2.16E-03	P14530.3	1
	snake venom metalloproteinase trimerelysin-II	3.12E-03	P20165.3	1
DI	disintegrin CTF-II	4.91E-07	P23323.1	3
	cytotoxic factor	9.96E-08	AAB19943.1	1
	disintegrin triflavin	4.67E-04	P21859.1	1
LAAO	L-amino acid oxidase	1.21E-06	BAP39950.1	1
	L-amino acid oxidase	1.28E-04	BAN82013.1	1
CTL	coagulation factor IX/X-binding protein	1.21E-06	1IXX_F	1
BPP related	Bradykinin-potentiating and C-type natriuretic peptides	4.93E-06	BAP39952.1	1
CRISP	CRISP Family Ca-Channel Blocker	7.52E-05	1WVR_A	1

2.2. Bottom-up analysis

Preprints (www.preprints.org) | NOT PEER-REVIEWED | Posted: 6 July 2018 doi:10.20944/preprints201807.0123.v1

Peer-reviewed version available at Molecules 2018, 23, 1893; doi:10.3390/molecules23081893

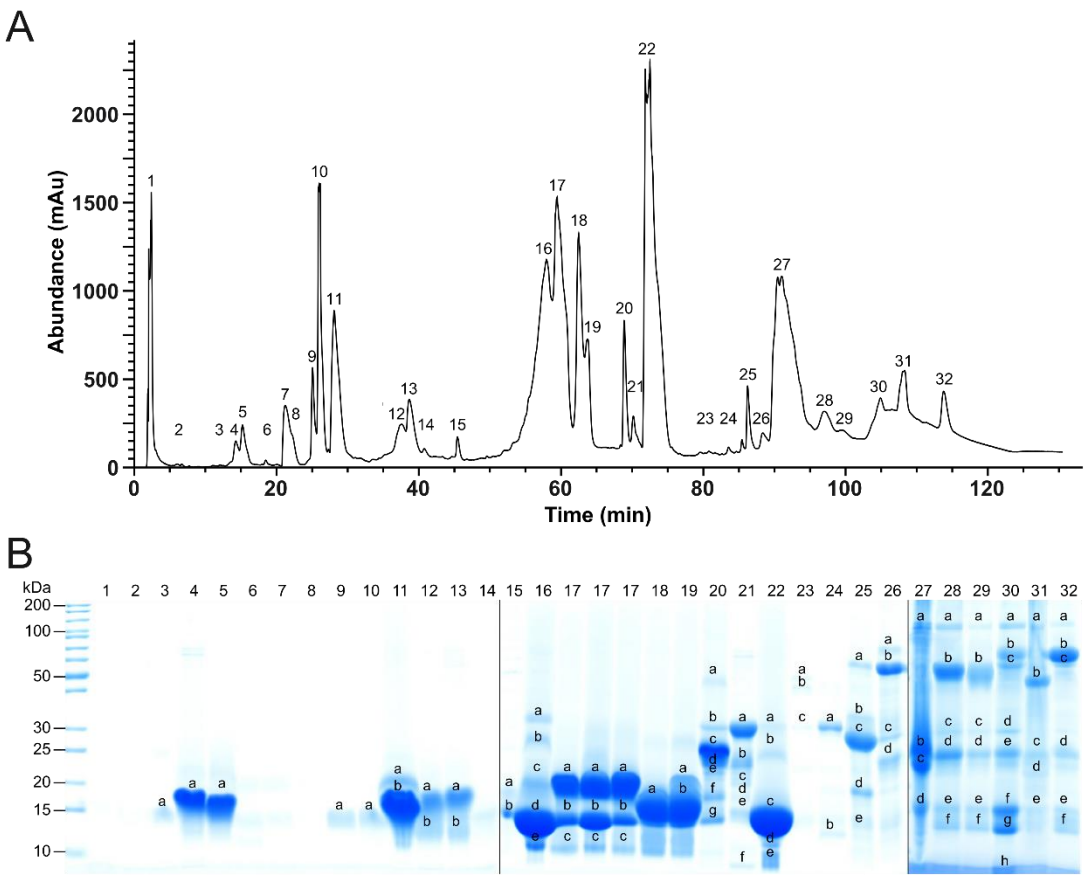

Figure 2. HPLC *P. flavoviridis* venom profile and fractions separate by SDS-PAGE. (A) Crude venom from *P. flavoviridis* was separated on a Supelco Discovery BIO wide Pore C18-3 RP-HPLC column and components were detected at λ=214 nm. Collected fractions (assigned above the correlated peaks), were dried, (B) separated by SDS-PAGE under reducing conditions (Coomassie staining). Alphabetically marked bands per line were excised for a subsequent tryptic in-gel digestion.

The TD approach gave a first and quick overview of lower molecular mass peptides and proteins, even of less prominent components, as constituents of the venom. A severe limitation of the TD approach however, is that proteins beyond a molecular mass of ~30 kDa are hardly detectable. This requires complementary analytics by a bottom-up approach: HPLC fractionation (Figure 2A) of the venom is followed by SDS-PAGE (Figure 2B) and a tryptic in-gel digest of protein bands. The subsequent MS *de novo* sequencing and semi-quantitative analysis led to the identification of the following toxin families: 55.1% phospholipases A_2 (PLA_2), 31.3% snake venom metalloproteinases and disintegrins (svMP/DI), 2.8% C-type lectin-like proteins (CTL), 1.8% cysteine-rich secretory proteins (CRISP), 1.4% snake venom serine proteases (svSP), 0.7% L-amino acid oxidases (LAAO), 0.07% phosphodiesterase (PDE) and 0.02% 5′-nucleotidase (5′-N). While 6.4% of the venom was assigned to peptides, 0.3% could not be annotated (n/a) (Figure 3).

Preprints (www.preprints.org) | NOT PEER-REVIEWED | Posted: 6 July 2018 doi:10.20944/preprints201807.0123.v1

Peer-reviewed version available at Molecules 2018, 23, 1893; doi:10.3390/molecules23081893

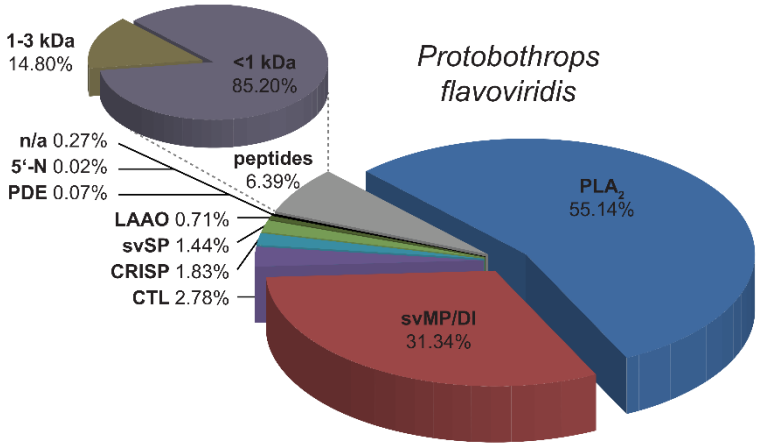

Figure 3. Semi-quantitative venom composition of *P. flavoviridis*. Relative occurrence of different toxin families and peptide content of *P. flavoviridis*: phospholipases A_2 (PLA_2, blue), snake venom metalloproteinases and disintegrins (svMP/DI, red), C-type lectin-like proteins (CTL, violet), cysteine rich secretory proteins (CRISP, light blue), snake venom serine proteases (svSP, light green), L-amino acid oxidases (LAAO, dark green). Less abundant are phosphodiesterases (PDE), 5'-nucleotidases (5'-N) and some unidentified proteins (n/a) (combined in black and peptides in grey). Groups of different peptide sizes are summarized in an additional pie chart percental related to the total peptide content. They were clustered to <1 kDa (dull purple) and 1-3 kDa (dull brown) parts.

According to the above findings, from components of the venom the phospholipase A_2 class formed the biggest part and includes the three most abundant proteins of the whole venom: The highest protein content belongs to the acidic PLA_2 1 (16.6%) eluting as fraction 22. Secondly, the basic PLA_2 BP (10.4%) was identified in fraction 16 but could not clearly be assigned as BPI or BPII, because of their high similarity, which differs only in a N58D exchange as a single mutation [45]. The third protein is PLA-N(O) (7.9%) of fraction 17, which is a PLA-N K121N isoform (Uniprot-ID: S6BAM8) previously documented for the *P. flavoviridis* population at Okinawa Island [15].

The svMP and DI members were detected at early retention times (HPLC fractions 4 and 5), but also formed the dominating protein classes at later retention times (fractions 27, 28, 32) (Table S1). Because svMP could include DI domains, both toxin families were combined in the final composition as the svMP/DI part thus forming the second most abundant group. The annotated sequences from fraction 4-13 belong to svMP P-II disintegrin domains, but with ~15 kDa, the observed molecular masses determined from the SDS gel appear too low for svMP P-II (expected molecular masses 30-60 kDa) and too high for single disintegrins (7-8 kDa). It is conceivable, that the identified disintegrin domains originate from degraded P-II or P-III metalloproteinases and contain neighboring sequence parts. This could mean, that the Habu venom contains truncated or auto-digested versions of svMP P-II or P-III, which is also known from other svMPs [44]. This autolysis was firstly observed for the two svMPs HR1A and HR1B isolated from the *P. flavoviridis* venom [46,47].

The CRISPs represent a minor part of the venom (1.8%) and were only found in fractions 20 and 21. The BU annotated triflin revealed in the IMP a molecular mass of 24767 Da with a -16 Da shift to the expected 24783 Da. The transcriptomic data of *P. flavoviridis* includes another CRISP (Uniprot-ID: T2HP25), which amino acid sequence differs from triflin (Uniprot-ID: Q8JI39) in two mutations: D110N and I113V. This isoform has an average molecular mass of 24768 Da and would correspond to our observation. To our knowledge, this proteoform, herein termed triflin-II, has not yet been described at the proteomic level.

Table 2. Identification of several venom isoforms by mass comparison. The bottom-up method (BU) in combination with the intact mass profiling (IMP) leads to a database-oriented identification of the isoforms in the crude venom. The theoretical mass includes oxidized cysteines for predicted Cys-Cys bridges. Asterisked entries mark the general identification as member of the according family.

Preprints (www.preprints.org) | NOT PEER-REVIEWED | Posted: 6 July 2018 doi:10.20944/preprints201807.0123.v1

Peer-reviewed version available at Molecules 2018, 23, 1893; doi:10.3390/molecules23081893

Fraction	Toxin family	Isoform identity by		UniProt-ID	Average mass in Da	
		BU	IMP	for IMP	observed	theoretical
16	PLA_2	BPII	BPII	P0DJJ9	13752.4	13752.1
			BPI	P0DJJ8		13753.1
17	PLA_2	PLA*	PLA-N(O)	S6BAM8	14020.2	14019.2
18	PLA_2	PLA*	PL-Y	Q90Y77	13944.3	13945.2
20	CRISP	triflin	triflin-II	T2HP25	24767.2	24767.9
22	PLA_2	PLA_2 1	PLA_2 1	P06859	13764.0	13764.6
25	svSP	flavoxobin	flavoxobin	P05620	25686.4	25687.4

Another protein validated by its molecular mass is the flavoxobin (Uniprot-ID: P05620), that belongs to the low abundant svSP family. This thrombin-like protease is the main part of fraction 25 and with 0.8% represents more than half of the svSP venom content, followed by svSP2 (Uniprot-ID: O13057) with 0.3%. In summary, the combination of three mass spectrometric methods, BU, TD and IMP led to the annotation of specific isoforms (Table 2).

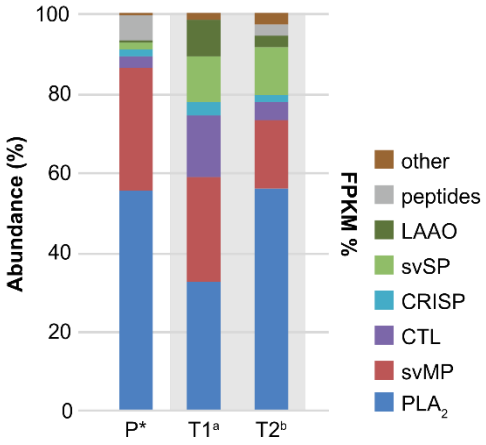

Figure 4. Proteomic and transcriptomic venom data of *P. flavoviridis*. Venom compositions of one proteomic analysis (P; quantified at 214 nm) and two venom gland transcriptomic analyses (T1 and T2) in fragments per kilobase million (FPKM %). The asterisked data set P is the result of this study. "Other" represents in all three data phosphodiesterases, 5'-nucleotidases and not annotated components. In the case of T1 and T2 additionally, galactose-binding lectins, nerve growth factors, phospholipases B, glutaminyl cyclases, vascular endothelial growth factor-like proteins as well as further less abundant detected families with <0.01% are included. The origins of toxin ratios are marked alphabetically: a [38], b [29].

In contrast to the herein presented proteomic data two previous transcriptomic compositions are known from the Habu by mRNA analysis of the venom glands [29,38]. They exhibit small analogies between the protein abundances and the fragments per kilobase million (FPKM %) of the main toxin families, but also remarkable differences regarding the proportional distribution (Figure 4). Both transcription analyses (T1, T2 in Figure 4) show PLA_2 as the highest expressed gene family followed by svMP which coincides with our proteomic data (P1 in Figure 4). On the other hand in T1 the PLA_2s form ~30%, while the amounts of P and T2 are comparable (~55%). With 17.3% the svMP gene expressions of T2 is lower than T1 and the protein amounts identified in the proteome (~30%). Interestingly, the proteomic and transcriptomic compositions correlate in lower represented groups: CRISP (2-4%), PDE (0.2-0.1%). In the other three families (CTL, svSP, LAAO), our measured proteomic levels are much lower than on the mRNA level. The data shows for CTL an up to five-fold,

and for svSP an eight-fold higher expression compared to the protein levels found. There is a considerable difference between the observed 0.7% of LAAOs in our study and T1 as well as T2, that show a four to 13-fold higher amount accounting for up to 9.1% of the complete transcriptome. Due to the fact that modern analysis can detect small amounts of RNA, very low concentrated targets can usually be observed, but not necessarily would be visible in proteomic approaches. All three studies identified PDEs and 5'-nucleotidases with abundances >0.2%. In the case of T1 and T2 further families in a range of 0.65-0.01% were observed but not in the venomic proteome P: galactose-binding lectins, nerve growth factors, phospholipases B, glutaminyl cyclases, vascular endothelial growth factor-like proteins, as well as further lesser abundant detected families with <0.01% of the total transcript abundance [29,38]. This underlines that reflecting the individual proteomic and transcriptomic compositions could not be easily compared between independent venom analyses of a species. Similarly, this has also been shown in studies on other members of *Viperidae* and *Elapidae* [48–50]. However, these two approaches in combination mutually represent a powerful handle for protein annotation and identification.

2.3. Bradykinin-potentiating peptides and snake venom metalloproteinase inhibitors

Besides the previously mentioned protein families, various bradykinin-potentiating peptides (BPP) and snake venom metalloproteinases inhibitor (svMP-i) are further constituents of snake venoms. The strong vasoactive effect of bradykinin, a substrate of the angiotensin-converting enzyme, was discovered in the late 1940's studying the *Bothrops jararaca* venom and exemplifies that research on snake venoms can lead to impressive developments in the drug development field [51,52]. The identification of a small peptide in the same venom, which increased effects of Kinin, was the first BPP [53] .This facilitated the design of hypertension drugs based on the structure of a snake toxin structure [54]. Today a multitude of different snake BPPs are known, and with the progress in the field of venomics, this number is still increasing.

By means of TD and IMP analytics, in total we identified 5 different BPP-RP bearing an N-terminal pyro-glutamate (pE): pEQWMPGGRPPHHIPP (Figure S1) and pESKPGRSPPISP (Figure S2). Until now the presence of both peptides was only hypothesized by transcriptomic data on *P. flavoviridis* [38,55].

In the peak of the BPP pESKPGRSPPISP (peak 5, Figure S1) by means of MS/MS two C-terminally truncated versions were identified: the 11mer peptide pESKPGRSPPIS (Figure S3) and the 10mer pESKPGRSPPI (Figure S4). Comparable to peptide pEQWMPGGRPPHHIPP the pEQWSQGRPR peptide (Figure S5) of peak 2 shows, a trimeric N-terminal sequence (pEQW), which as tripeptide, is known for its inhibition of svMP.

To minimize the risk of a self-degradation by metalloproteinases also present in high concentrations in the herein studied venom, snakes secret small trimeric peptides. These svMP inhibitors are processed from the same precursor like the BPPs and also contain an N-terminal pyroglutamate [56]. In summary, we could identify three different svMP-is, that represent the main components of the TIC: peak 4 (pEKW, *m/z* 444.22), peak 6 (pENW, *m/z* 430.17) and peak 7 (pEQW, *m/z* 444.18) (Figure S6-8). Another prominent molecular mass signal beneath the main peak *m/z* 444.18 was detected at *m/z* 427.13 and could be identified as pEEW which is the deaminated form of peak 7 pEQW (Figure S9). Previously, these three svMP-is were further isolated from the Taiwan Habu (*Trimeresurus mucrosquamatus*), a closely related pit viper of the herein investigated *P. flavoviridis*, and revealed there strong inhibitory activity [57].

2.4. Cytotoxicity test

Table 3. IC_{50} values of *P. flavoviridis* venom against human cell lines. The half maximal inhibitory concentrations (IC_{50} in µg/mL) were determined for the crude venom of *P. flavoviridis* against one non-cancerous (HEK-293) and six cancerous human cell lines. Error mean in ±SD.

Cell line	*P. flavoviridis*	Doxorubicin
	IC_{50} values in µg/mL	IC_{50} values in µg/mL

Preprints (www.preprints.org) | NOT PEER-REVIEWED | Posted: 6 July 2018 doi:10.20944/preprints201807.0123.v1

Peer-reviewed version available at Molecules 2018, 23, 1893; doi:10.3390/molecules23081893

HEK-293	1.02 ± 0.02	0.002±0.001
SH-SY5Y	4.68 ± 0.92	0.06±0.02
MDA-MB-231	22.84 ± 2.51	4.98±0.28
A549	38.51 ± 0.13	1.03±0.37
PANC1	>50	0.05±0.01
HeLa	24.78 ± 0.77	1.03±0.25
PC-3	51.55 ± 2.79	2.02±0.46

The snake venom of *P. flavoviridis* is well known to cause strong cytotoxic effects and various isolated toxins, e.g. LAAO OHAP-1 in glioma cells [58,59], exhibit *in vivo* apoptotic activities. The Habu venom was monitored in this study against several human cancer cell lines and therefore, the cytotoxicity was determined for cancerous (SH-SY5Y, MDA-MB-231, A549, PANC1, HeLa, PC-3) as well as non-cancerous (HEK293) cells by the MTT assay. The IC_{50} values range from ~1 to >50 µg/mL (Table 3).

Table 4. IC_{50} values of *P. flavoviridis* venom fractions against SH-SY5Y cells. Single RP-HPLC venom fractions of *P. flavoviridis* were tested against human neuroblastoma SH-SY5Y cells and the half maximal inhibitory concentrations (IC_{50} in µg/mL) were determined. Doxorubicin was used as reference and error mean in ±SD.

HPLC Fraction	IC_{50} in µg/mL
6	0.680 ± 0.002
7	4.60 ± 0.24
8	9.19 ± 1.22
9/10	0.87 ± 0.05
12	49.63 ± 2.46
13	45.46 ± 7.45
15	17.94 ± 2.96
16	4.02 ± 0.24
17	2.18 ± 0.12
18	30.57 ± 1.50
19	23.96 ± 2.55
20	38.82 ± 2.82
21	17.25 ± 0.98
22	15.57 ± 1.10
Doxorubicin	0.83 ± 0.20

The highest inhibition of proliferation was found against HEK293 (1.02 µg/mL) and SH-SY5Y (4.7 µg/mL) cells (Figure S11). SH-SY5Y as most sensitive cancer cell line has been selected for further screenings with single RP-HPLC venom fractions. While various tested fractions were found to be active, fractions 6 and 9/10 were the most effective with IC_{50} values of 0.7 and 0.9 µg/mL (Table 4). The main compound of the most active fraction 6 is the svMP-i pENW, while the pEQW containing fraction 7 less cell toxic (4.6 µg/mL). According to this cytotoxicity results, the *P. flavoviridis* venom svMP-i exhibits remarkable effects on SH-SY5Y cells, while until now only the correlating svMP of most *Protobothrops* venoms were known for their important role in envenomation-related pathologies [46,60]. Regarding the identified families, PLA_{2}s as main venom part are most active in fractionss 15 (PLA-N(O), 2.2 µg/mL) and 14 (PLA_2 BP-I/II, 4.0 µg/mL), against neuroblastoma cells. An induced caspase-independent apoptosis by the PLA_2 BP-II in leukemia cell was previously shown [58]. The

other PLA2 fractions (16, 17, 20, and 22) as well as the CRISP triflin-II fraction 21 and the svSP of fraction 22 show a moderate cytotoxicity (16 to 30 µg/mL). The SH-SY5Y cytotoxic effect of the most active fraction 6 and 9/10 is shown by microscopic imaging (Figure 5) as well as of all tested fractions in overview with different concentrations (Figure 12). Furthermore, fraction 9/10 and 13-15 against SH-SY5Y cells indicates at higher concentrations a disintegrine-like conglomeration effect (Figure S12), that correlate with the observation of svMP/DI in these fractions by BU, IMP and the TD, like the disintegrin CTF-II proteoform (Table S1). Future studies will focus on the mechanism of the *P. flavoviridis* venom action in SH-SY5Y cells, especially due to DI and svMP-i.

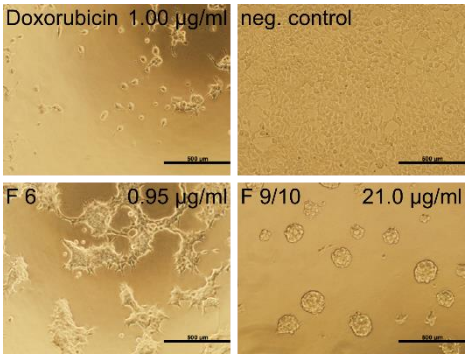

Figure 5. Most active *P. flavoviridis* venom fraction treatment of SH-SY5Y cells. Single RP-HPLC venom fraction 6 and 9/10 of *P. flavoviridis* with the mentioned concentration in µg/mL were tested against human neuroblastoma SH-SY5Y cells. Imaged were taken after 48 h treatment at 37 °C. Doxorubicin was used as positive cytotoxic control drug and no stimulation as negative control.

3. Discussion

In this contribution we report on the first quantitative mass spectrometry-guided proteomic snake venom analysis of the Japanese pit viper *P. flavoviridis*. The combination of all three mass spectrometric methods (BU, TD and IMP) facilitates the annotation of isoforms, respectively based on databases even without the full sequencing of every protein. The combined data reveal PLA2s (55.1%) as major part of the venom, with PLA2 1, PLA2 BP I/II and PLA-N(O) as main representatives. Following by the svMP/DI group and several minor represented toxins families, like the svSP with flavoxobin and svSP2. For the first time a CRISP triflin-homolog, named triflin-II, was observed at the proteomics level. The top-down approach to identify proteins as well as peptides, was reliable for toxins with molecular masses up to ~30 kDa. Venom compounds in a range of *m/z* 338.1 to 30384.7 were detected by the intact mass profiling with the same restrictions for high masses like the top-down, while the SDS-PAGE exhibits proteins till over 100 kDa. Additionally, cytotoxicity assays of whole and fractionated crude venom reveal promising results against SH-SY5Y neuroblastoma cells.

4. Materials and Methods

4.1. Sample preparation and system setup

The pooled Habu venom of six *P. flavoviridis* specimen (four females, two males) was purchased from the Kentucky Reptile Zoo (Slayde, KY, USA) and kindly provided by Professor Dr. Johannes A. Eble (University of Münster, Germany). The crude venom (final concentration 10 mg/mL) was dissolved in 10 µl HFo (1% (v/v)) and centrifuged at 20,000 xg for 5 min. Then 30 µL of citrate buffer (0.1 M, pH 4.3) was added. One half of the sample (20 µL) was chemically reduced by adding 10 µL of 0.5 M *tris*(2-carboxyethyl)-phosphine (TCEP) and incubated for 30 min at 65 °C, while 10 µL ultra-pure water was added to the other half, as non-reduced/native sample. All samples were centrifuged at 20,000 xg for 5 min and submitted to IMP (native) and TD venomics (native, reduced): HPLC-high-resolution (HR) ESI-MS/MS measurements were performed on a LTQ Orbitrap XL mass spectrometer (Thermo, Bremen, Germany) coupled to an Agilent 1260 HPLC system (Agilent, Waldbronn, Germany) using a Supelco Discovery 300 Å C18 (2 x 150 mm, 3 µm particle size) column. The elution

was performed by a gradient of ultra-pure water with 0.1% formic acid (HFo) (v/v; buffer A) and acetonitrile (ACN) with 0.1% HFo (v/v; buffer B) at a flow rate of 1 mL/min. An isocratic equilibration (5% B) for 5 min was followed by a linear gradient of 5-40% B for 95 min, 40-70% B for 20 min, 70% B for 10 min and a re-equilibration with 5% B for 10 min.

ESI settings were: 11 L/min sheath gas, 35 L/min auxiliary gas, spray voltage 4.8 kV, capillary voltage 63 V, tube lens voltage 135 V, and capillary temperature 330 °C. The data-dependent acquisition (DDA) mode was used for MS/MS experiments with 1 µ scans and 1000 ms maximal fill time. The precursor ions were selected with a range of ±2 *m/z* and after two repeats within 10 s excluded with ±3 *m/z* for duration of 20 s. Three scan events were performed with a normalized CID energy of 30%, 35% and a HCD with 35% collision energy.

4.2. Intact mass profiling (IMP)

For IMP, the mass spectrometric data were inspected via the Xcalibur Qual Browser (Thermo Xcalibur 2.2 SP1.48) and the deconvolution of isotopically resolved spectra was carried out by using the XTRACT algorithm of Xcalibur Qual Browser. The protein assignment was done by comparison with the retention times obtained from the HPLC runs. Sequence annotations and molecular mass comparisons to protein database entries of *P. flavoviridis* (taxid: 88087) were performed manually.

4.3. Top-down (TD) venomics

The top-down analytical data were obtained based on the protocol of Petras et al., 2016 [61] with the following alterations: data were inspected with the Qual Browser (Thermo Xcalibur 2.2 SP1.48) and prepared based on the TopPIC workflow. The .raw data was converted to a centroided .mzXML using MSconvert of the ProteoWizard package (http://proteowizard.sourceforge.net) version 3.0.10577. The .mzXML data was deconvoluted to an .msalign file using MS-Deconv (http://bix.ucsd.edu/projects/msdeconv) version 0.8.0.7370 (maximum charge 30, maximum mass 50,000, *m/z* tolerance 0.02, s/n ratio 1.0). The final sequence annotation was performed by TopPIC (http://proteomics.informatics.iupui.edu/software/toppic/) version 1.0.0 with a targeted search type, error tolerance 15 ppm and an E-value cutoff at 0.01 by E-value computation.

Variable modifications were acetylation of Lys (+42.010565 Da), phosphorylation of Ser, Thr and Tyr (+79.966331 Da), oxidation of Met (+15.994915 Da), N-terminal methylation (+14.015650 Da), N-terminal pyro-Glu formation of Glu (-18.010565 Da) and Gln (17.026549 Da), N-acetylhexoseamine formation of Arg (HexNAc +203.079373 Da) and in the case of non-reduced samples a dehydrogenation of Cys (-1.007825 Da for each Cys) rendering Cys-Cys bridges. A maximum of two unexpected modifications was allowed with a 500 Da maximal mass.

The sequences were matched against a protein NCBI database of *P. flavoviridis* (taxid: 88087, 852 entries, 8th September 2017), manual validated and graphical visualized using the MS and MS/MS spectra of the Xcalibur Qual Browser.

4.4. Bottom-up (BU) venomics

Lyophilized crude venom (4 mg) was dissolved to a final concentration of 20 mg/mL in aqueous 3% (v/v) ACN with 1% (v/v) HFo. The solution was centrifuged at 20,000 xg for 5 min and the supernatant was loaded onto a semi-preparative reversed-phase HPLC with a Supelco Discovery BIO wide Pore C18-3 column (4.6 x 150 mm, 3 µm particle size) using an Agilent 1260 Low Pressure Gradient System (Agilent, Waldbronn, Germany). As gradient buffer ultra-pure water with 0.1% (v/v) HFo (buffer A) and ACN with 0.1% (v/v) HFo (buffer B) were used with a flow rate of 1 mL/min. An isocratic equilibration (5% B) for 5 min was followed by the toxin elution with a linear gradient of 5-40% B for 95 min, 40-70% B for 20 min and 70% B for 10 min.

Absorbance was measured at λ=214 nm using a DAD detector and 1 mL fractions were automatically collected. Peaks of the chromatograms were manually pooled and vacuum dried (Thermo Speedvac, Bremen, Germany). Fractions were submitted to SDS-PAGE under reducing conditions [62]. Coomassie (Blue G250, Serva, Heidelberg, Germany) stained protein bands were cut,

Peer-reviewed version available at *Molecules* **2018**, *23*, 1893; doi:10.3390/molecules23081893

in-gel reduced with fresh dithiothreitol (100 mM DTT in 100 mM ammonium hydrogencarbonate, pH 8.3, for 30 min at 56 °C) and alkylated with fresh iodoacetamide (55 mM IAC in 100 mM ammonium hydrogencarbonate, pH 8.3, for 20 min at 25 °C). An in-gel trypsin (Thermo, Rockfeld, IL, USA) digestion was performed (6.7 ng/µL in 10 mM ammonium hydrogencarbonate with 10% (v/v) ACN, pH 8.3, for 18 h at 37 °C with 0.27 µg/band). The peptides were extracted with 100 µL aqueous 30% (v/v) ACN with 5% (v/v) HFo for 15 min at 37 °C, the supernatants were vacuum dried, re-dissolved in 20 µL aqueous 3% (v/v) ACN with 1% (v/v) HFo and submitted to LC-MS/MS analysis.

The analytics of tryptic peptides was performed using a reversed-phase Grace Vydac 218MSC18 column (2.1 x 150 mm, 5 µm particle size) under control of an Agilent 1260 HPLC system (Agilent Technologies, Waldbronn, Germany). The HPLC separation was operated with a flow rate of 0.3 mL/min. After an isocratic equilibration (5% B) for 1 min, the peptides were eluted with a linear gradient of 5-40% B for 10 min, 40-99% B for 3 min, washed with 99% B for 3 min and re-equilibrated in 5% B for 3 min.

MS experiments were performed on an Orbitrap XL mass spectrometer (Thermo, Bremen, Germany) with R=15,000 at *m/z* 400 and maximum filling time of 200 ms for first product ion scans. MS/MS fragmentation of the most intense ion was performed in the LTQ using a collision-induced dissociation (30 ms activation time); the collision energy was set to 30% and 35%. The precursor ions were selected with a range of ±2 *m/z* and after two repeats within 10 s excluded with ±3 *m/z* for duration of 20 s.

LC-MS/MS data files (.raw) were converted to mgf files via MSConvert GUI of the ProteoWizard package (http://proteowizard.sourceforge.net; version 3.0.10577) and annotated by DeNovo GUI 1.15.11 [63] with carbamidomethylated cysteine (+57.021464 Da) as fixed modification. Variable modifications were acetylation of lysine (+42.010565 Da) and phosphorylation of serine and threonine (+79.966331 Da).

The peptide sequences were matched against a non-redundant protein NCBI database of *P. flavoviridis* (taxid: 88087) using BLASTP (http://blast.ncbi.nlm.nih.gov).

4.5. Relative toxin quantification

Thepercentage composition of the venom ingredients was calculated on the basis of a combination of the RP-HPLC chromatogram and SDS-PAGE evaluation [64,65]. The peak integrals at UV_{214nm} were measured in comparison to the total sum of peak integrals. In the case of multiple component elution in an HPLC fraction identified by SDS-PAGE staining, the integrated density ratio of the stained bands was respectively used for emphasis of peak integrals.

4.6. Data accessibility

Mass spectrometry proteomics data (.mgf, .raw and output files) have been deposited at the ProteomeXchange Consortium [66] (http://proteomecentral.proteomexchange.org) via the MassIVE partner repository under the project name "Venomics of the Okinawa Habu pit viper *Protobothrops flavoviridis*" and data set identifier PXD009414.

4.7. Cell culture and in vitro *cytotoxicity assay*

Human cells were purchased from ATCC (Manassas, VA, USA) and cultivated in Dulbecco's modified Eagle's medium F-12 (DMEM/F-12, 10% fetal bovine serum (FBS), 2 mM/L glutamine, 100 U/mL penicillin, 100 mg/mL streptomycin) (Gibco, Carlsbad, CA, USA). The following cell lines were used: HEK-293 (human embryonic kidney), SH-SY5Y (neuroblastoma), MDA-MB-231 (breast epithelial adenocarcinoma), A549 (human alveolar adenocarcinoma), PANC1 (pancreas adenocarcinoma), HeLa (human cervix adenocarcinoma) and PC-3 (human prostate adenocarcinoma). *In vitro* cytotoxicity assays were performed with crude venom and HPLC fractions by using a modified 3-(4,5-dimethyl-2-thiazolyl)-2,5-diphenyl-2H-tetrazoliumbromide) (MTT). The protein concentrations in saline were estimated by using a BCA protein assay kit (Thermo-Scientific, Darmstadt, Germany) with a 595 nm ultraviolet (UV)-visible spectrophotometer (VersaMax,

Peer-reviewed version available at *Molecules* **2018**, *23*, 1893; doi:10.3390/molecules23081893

Molecular Devices, San Jose, CA, USA). Bovine serum albumin was used as a standard for calibration line.

A modified MTT assay was used to determine the cytotoxicity of the snake venom. Therefore, 1x10^5 cells/mL were seeded in 96-well microtiter plated. After 24 h cultivation the cells were treated for 48 h at 37 °C with crude venom, venom fractions or doxorubicin as positive cytotoxic control drug.

The optical density (OD) was measured in triplicates at λ=570 nm (with a reference wavelength of λ=690 nm) by UV/Vis spectrophotometry (Thermo, Bremen, Germany). The cell viability was determined with an absorbance A:

$$\text{Viable cells} = \frac{A_{\text{treated}} - A_{\text{blank}}}{A_{\text{untreated}} - A_{\text{blank}}} \cdot 100$$

4.8. Morphological studies

The morphological changes of the cells following treatment with crude venom or single RP-HPLC venom fractions of *P. flavoviridis* were observed under an inverted microscope (Olympus, Toyo, Japan) compared to the control group following a 48 h treatment.

4.9. Half maximal inhibition of growth (IC50) determination

The half maximal inhibition of growth (IC_{50}) were calculated based on a sigmoidal curve fitting using a four-parameter logistic model in comparison to untreated controls in Prism 5 software (GraphPad5, San Diego, CA, USA). Values are presented at 95% confidence interval and as average of three independent measurements.

Supplementary Materials: The following are available online at www.mdpi.com/xxx/s1, Figure S1-S5: Annotated MS2 spectra of BPP-RP, Figure S6-S9: Annotated MS2 spectra of tripeptidic svMP-i, Figure S101: *P. flavoviridis* reduced venom MS TIC for IMP and TD, Figure S11: *P. flavoviridis* venom tested for cytotoxicity against different human cell lines, Figure S12: SH-SY5Y cells after 48 h treatment with different *P. flavoviridis* venom fractions.

Author Contributions: M.D., B.-F.H., A.N. and R.D.S. conceived and designed the experiments, M.D., B.-F.H. performed and analyzed the proteomic experiments and data, A.N. performed and analyzed the cytotoxicity experiments and data. All authors contributed reagents/materials/analysis tools, M.D., B.-F.H., A.N. and R.D.S wrote the paper. All contributors critically read and revised the manuscript.

Funding: to fill with TU text

Acknowledgments: We thank in specially Prof. Dr. Johannes A. Eble from the University Münster in Germany for providing the venom of *Protobothrops flavoviridis*. Further we would like to thank Shawn Miller for providing us with images of the Okinawa Habu snake (*Trimeresurus flavoviridis*).

Conflicts of Interest: The authors declare no conflict of interest.

References

1. Antoniou, S.A.; Antoniou, G.A.; Learney, R.; Granderath, F.A.; Antoniou, A.I. The rod and the serpent: History's ultimate healing symbol. *World journal of surgery* **2011**, *35*, 217–221, [10.1007/s00268-010-0686-y].
2. Stanley, J.W. Snakes: Objects of Religion, Fear and Myth. *Elec. J. Integr. Biol.* **2008**, *2*, 61-76.
3. Retief, F.P.; Cilliers, L. Snake and staff symbolism, and healing. *South African medical journal = Suid-Afrikaanse tydskrif vir geneeskunde* **2002**, *92*, 553–556.
4. Wake, C.S. The Origin of Serpent-Worship. *The Journal of the Anthropological Institute of Great Britain and Ireland* **1873**, *2*, 373, [10.2307/2841458].
5. Chippaux, J.-P. Snakebite envenomation turns again into a neglected tropical disease! *J Venom Anim Toxins Incl Trop Dis* **2017**, *23*, 515, [10.1186/s40409-017-0127-6].
6. Tanaka, K.; Mori, A. Literature Survey on Predators of Snakes in Japan. *Curr.Herpetol.* **2000**, *19*, 97–111, [10.5358/hsj.19.97].

7. Yasunaga, H.; Horiguchi, H.; Kuwabara, K.; Hashimoto, H.; Matsuda, S. Short report: Venomous snake bites in Japan. *The American journal of tropical medicine and hygiene* **2011**, *84*, 135–136, [10.4269/ajtmh.2011.10-0403].
8. Tandavanitj, N.; Ota, H.; Cheng, Y.-C.; Toda, M. Geographic genetic structure in two laticaudine sea kraits, *Laticauda laticaudata* and *Laticauda semifasciata* (Serpentes *Elapidae*), in the Ryukyu-Taiwan region as inferred from mitochondrial cytochrome b sequences. *Zoological science* **2013**, *30*, 633–641, [10.2108/zsj.30.633].
9. Morokuma, K.; Kobori, N.; Fukuda, T.; Uchida, T.; Sakai, A.; Toriba, M.; Ohkuma, K.; Nakai, K.; Kurata, T.; Takahashi, M. Experimental manufacture of equine antivenom against yamakagashi (*Rhabdophis tigrinus*). *Japanese journal of infectious diseases* **2011**, *64*, 397–402.
10. Schneider-Poetsch, T.; Takahashi, S.; Jang, J.-H.; Ahn, J.S.; Osada, H. Eighth Korea-Japan Chemical Biology symposium: Chemical biology notes from a small island. *The Journal of antibiotics* **2016**, *69*, 885–888, [10.1038/ja.2016.58].
11. Somaweera, R.; Somaweera, N. Serpents in jars: The snake wine industry in Vietnam. *J. Threat. Taxa* **2010**, *2*, 1251–1260, [10.11609/JoTT.o2361.1251-60].
12. Moon, J.M.; Chun, B.J. Severe Coagulopathy after Ingestion of "Snake Wine". *The Journal of emergency medicine* **2016**, *50*, 848–851, [10.1016/j.jemermed.2015.11.037].
13. Tu, M.C.; Wang, H.Y.; Tsai, M.P.; Toda, M.; Lee, W.J.; Zhang, F.J.; Ota, H. Phylogeny, taxonomy, and biogeography of the oriental pitvipers of the genus *trimeresurus* (*reptilia*: *viperidae*: *crotalinae*): a molecular perspective. *Zoological science* **2000**, *17*, 1147–1157, [10.2108/zsj.17.1147].
14. Shibata, H.; Chijiwa, T.; Hattori, S.; Terada, K.; Ohno, M.; Fukumaki, Y. The taxonomic position and the unexpected divergence of the Habu viper, *Protobothrops* among Japanese subtropical islands. *Molecular phylogenetics and evolution* **2016**, *101*, 91–100, [10.1016/j.ympev.2016.04.027].
15. Chijiwa, T.; Hamai, S.; Tsubouchi, S.; Ogawa, T.; Deshimaru, M.; Oda-Ueda, N.; Hattori, S.; Kihara, H.; Tsunasawa, S.; Ohno, M. Interisland mutation of a novel phospholipase A2 from *Trimeresurus flavoviridis* venom and evolution of Crotalinae group II phospholipases A2. *Journal of molecular evolution* **2003**, *57*, 546–554, [10.1007/s00239-003-2508-4].
16. Nishimura, H.; Enokida, H.; Kawahira, S.; Kagara, I.; Hayami, H.; Nakagawa, M. Acute Kidney Injury and Rhabdomyolysis After *Protobothrops flavoviridis* Bite: A Retrospective Survey of 86 Patients in a Tertiary Care Center. *The American journal of tropical medicine and hygiene* **2016**, *94*, 474–479, [10.4269/ajtmh.15-0549].
17. Hifumi, T.; Sakai, A.; Kondo, Y.; Yamamoto, A.; Morine, N.; Ato, M.; Shibayama, K.; Umezawa, K.; Kiriu, N.; Kato, H.*; et al.* Venomous snake bites: clinical diagnosis and treatment. *Journal of intensive care* **2015**, *3*, 16, [10.1186/s40560-015-0081-8].
18. Benard-Valle, M.; Neri-Castro, E.E.; Fry, B.G.; Boyer, L.; Cochran, C.; Alam, M.; Jackson, T.; Paniagua, D.; Olvera-Rodriguez, F.; Koludarov, I.*; et al.* Antivenom Research and Development. In *Venomous reptiles and their toxins*: *Evolution, pathophysiology, and biodiscovery*; Fry, B.G., Ed.: Oxford University Press: New York, NY, 2015, pp. 61–72.
19. Bochner, R. Paths to the discovery of antivenom serotherapy in France. *J Venom Anim Toxins Incl Trop Dis* **2016**, *22*, 20, [10.1186/s40409-016-0074-7].
20. Lomonte, B.; Calvete, J.J. Strategies in 'snake venomics' aiming at an integrative view of compositional, functional, and immunological characteristics of venoms. *J Venom Anim Toxins Incl Trop Dis* **2017**, *23*, 26, [10.1186/s40409-017-0117-8].
21. Aird, S.D. Taxonomic distribution and quantitative analysis of free purine and pyrimidine nucleosides in snake venoms. *Comparative biochemistry and physiology. Part B, Biochemistry & molecular biology* **2005**, *140*, 109–126, [10.1016/j.cbpc.2004.09.020].

22. Devi, A. The Protein and Nonprotein Constituents of Snake Venoms. In *Venomous Animals and Their Venoms*: *Venomous Vertebrates*, 1st ed; Bücherl, W., Buckley, E.E., Deulofeu, V., Eds.: Academic Press: New York, London, 1968; I, pp. 119–165.
23. Fry, B.G., Ed. *Venomous reptiles and their toxins*: *Evolution, pathophysiology, and biodiscovery*; Oxford University Press: New York, NY, 2015.
24. Mebs, D. *Gifttiere*: *Ein Handbuch für Biologen, Toxikologen, Ärzte und Apotheker*, 3rd ed; Wissenschaftliche Verlagsgesellschaft: Stuttgart, 2010.
25. Mackessy, S.P., Ed. *Handbook of venoms and toxins of reptiles*; CRC Press: Boca Raton, Fla., 2010.
26. Pimenta, D.C.; Prezoto, B.C.; Konno, K.; Melo, R.L.; Furtado, M.F.; Camargo, A.C.M.; Serrano, S.M.T. Mass spectrometric analysis of the individual variability of Bothrops jararaca venom peptide fraction. Evidence for sex-based variation among the bradykinin-potentiating peptides. *Rapid communications in mass spectrometry : RCM* **2007**, *21*, 1034–1042, [10.1002/rcm.2931].
27. Tasoulis, T.; Isbister, G.K. A Review and Database of Snake Venom Proteomes. *Toxins* **2017**, *9*, *[*10.3390/toxins9090290].
28. Fox, J.W.; Serrano, S.M.T. Exploring snake venom proteomes: Multifaceted analyses for complex toxin mixtures. *Proteomics* **2008**, *8*, 909–920, [10.1002/pmic.200700777].
29. Aird, S.D.; Aggarwal, S.; Villar-Briones, A.; Tin, M.M.-Y.; Terada, K.; Mikheyev, A.S. Snake venoms are integrated systems, but abundant venom proteins evolve more rapidly. *BMC genomics* **2015**, *16*, 647, [10.1186/s12864-015-1832-6].
30. Ogawa, T.; Chijiwa, T.; Oda-Ueda, N.; Ohno, M. Molecular diversity and accelerated evolution of C-type lectin-like proteins from snake venom. *Toxicon : official journal of the International Society on Toxinology* **2005**, *45*, 1–14, [10.1016/j.toxicon.2004.07.028].
31. Arlinghaus, F.T.; Eble, J.A. C-type lectin-like proteins from snake venoms. *Toxicon : official journal of the International Society on Toxinology* **2012**, *60*, 512–519, [10.1016/j.toxicon.2012.03.001].
32. Nakashima, K.; Ogawa, T.; Oda, N.; Hattori, M.; Sakaki, Y.; Kihara, H.; Ohno, M. Accelerated evolution of *Trimeresurus flavoviridis* venom gland phospholipase A2 isozymes. *Proceedings of the National Academy of Sciences of the United States of America* **1993**, *90*, 5964–5968.
33. Aoki, N.; Sakiyama, A.; Deshimaru, M.; Terada, S. Identification of novel serum proteins in a Japanese viper: homologs of mammalian PSP94. *Biochemical and biophysical research communications* **2007**, *359*, 330–334, [10.1016/j.bbrc.2007.05.091].
34. Arlinghaus, F.T.; Eble, J.A. The collagen-binding integrin $\alpha 2\beta 1$ is a novel interaction partner of the *Trimeresurus flavoviridis* venom protein flavocetin-A. *The Journal of biological chemistry* **2013**, *288*, 947–955, [10.1074/jbc.M112.399618].
35. Taniuchi, Y.; Kawasaki, T.; Fujimura, Y.; Suzuki, M.; Titani, K.; Sakai, Y.; Kaku, S.; Hisamichi, N.; Satoh, N.; Takenaka, T. Flavocetin-A and -B, two high molecular mass glycoprotein Ib binding proteins with high affinity purified from *Trimeresurus flavoviridis* venom, inhibit platelet aggregation at high shear stress. *Biochimica et biophysica acta* **1995**, *1244*, 331–338.
36. Atoda, H.; Hyuga, M.; Morita, T. The primary structure of coagulation factor IX/factor X-binding protein isolated from the venom of *Trimeresurus flavoviridis*. Homology with asialoglycoprotein receptors, proteoglycan core protein, tetranectin, and lymphocyte Fc epsilon receptor for immunoglobulin E. *The Journal of biological chemistry* **1991**, *266*, 14903–14911.
37. Nuyttens, B.P.; Thijs, T.; Deckmyn, H.; Broos, K. Platelet adhesion to collagen. *Thrombosis research* **2011**, *127 Suppl 2*, S26-9, [10.1016/S0049-3848(10)70151-1].

38. Aird, S.D.; Watanabe, Y.; Villar-Briones, A.; Roy, M.C.; Terada, K.; Mikheyev, A.S. Quantitative high-throughput profiling of snake venom gland transcriptomes and proteomes (*Ovophis okinavensis* and *Protobothrops flavoviridis*). *BMC genomics* **2013**, *14*, 790, [10.1186/1471-2164-14-790].
39. Calvete, J.J.; Petras, D.; Calderón-Celis, F.; Lomonte, B.; Encinar, J.R.; Sanz-Medel, A. Protein-species quantitative venomics: Looking through a crystal ball. *J Venom Anim Toxins Incl Trop Dis* **2017**, *23*, 27, [10.1186/s40409-017-0116-9].
40. Calvete, J.J.; Juárez, P.; Sanz, L. Snake venomics. Strategy and applications. *Journal of mass spectrometry : JMS* **2007**, *42*, 1405–1414, [10.1002/jms.1242].
41. Georgieva, D.; Arni, R.K.; Betzel, C. Proteome analysis of snake venom toxins: Pharmacological insights. *Expert review of proteomics* **2008**, *5*, 787–797, [10.1586/14789450.5.6.787].
42. Hempel, B.-F.; Damm, M.; Göçmen, B.; Karis, M.; Oguz, M.A.; Nalbantsoy, A.; Süssmuth, R.D. Comparative Venomics of the Vipera ammodytes transcaucasiana and Vipera ammodytes montandoni from Turkey Provides Insights into Kinship. *Toxins* **2018**, *10*, [10.3390/toxins10010023].
43. Göçmen, B.; Heiss, P.; Petras, D.; Nalbantsoy, A.; Süssmuth, R.D. Mass spectrometry guided venom profiling and bioactivity screening of the Anatolian Meadow Viper, *Vipera anatolica*. *Toxicon : official journal of the International Society on Toxinology* **2015**, *107*, 163–174, [10.1016/j.toxicon.2015.09.013].
44. Fox, J.W.; Serrano, S.M.T. Insights into and speculations about snake venom metalloproteinase (SVMP) synthesis, folding and disulfide bond formation and their contribution to venom complexity. *The FEBS journal* **2008**, *275*, 3016–3030, [10.1111/j.1742-4658.2008.06466.x].
45. Liu, S.Y.; Yoshizumi, K.; Oda, N.; Ohno, M.; Tokunaga, F.; Iwanaga, S.; Kihara, H. Purification and amino acid sequence of basic protein II, a lysine-49-phospholipase A2 with low activity, from *Trimeresurus flavoviridis* venom. *Journal of biochemistry* **1990**, *107*, 400–408.
46. Fox, J.W.; Serrano, S.M.T. Timeline of key events in snake venom metalloproteinase research. *Journal of proteomics* **2009**, *72*, 200–209, [10.1016/j.jprot.2009.01.015].
47. Takeya, H.; Nishida, S.; Nishino, N.; Makinose, Y.; Omori-Satoh, T.; Nikai, T.; Sugihara, H.; Iwanaga, S. Primary structures of platelet aggregation inhibitors (disintegrins) autoproteolytically released from snake venom hemorrhagic metalloproteinases and new fluorogenic peptide substrates for these enzymes. *Journal of biochemistry* **1993**, *113*, 473–483.
48. Aird, S.D.; da Silva, N.J.; Qiu, L.; Villar-Briones, A.; Saddi, V.A.; Pires de Campos Telles, M.; Grau, M.L.; Mikheyev, A.S. Coralsnake Venomics: Analyses of Venom Gland Transcriptomes and Proteomes of Six Brazilian Taxa. *Toxins* **2017**, *9*, [10.3390/toxins9060187].
49. Margres, M.J.; McGivern, J.J.; Wray, K.P.; Seavy, M.; Calvin, K.; Rokyta, D.R. Linking the transcriptome and proteome to characterize the venom of the eastern diamondback rattlesnake (*Crotalus adamanteus*). *Journal of proteomics* **2014**, *96*, 145–158, [10.1016/j.jprot.2013.11.001].
50. Greenbaum, D.; Colangelo, C.; Williams, K.; Gerstein, M. Comparing protein abundance and mRNA expression levels on a genomic scale. *Genome biology* **2003**, *4*, 117, [10.1186/gb-2003-4-9-117].
51. Camargo, A.C.M.; Ianzer, D.; Guerreiro, J.R.; Serrano, S.M.T. Bradykinin-potentiating peptides: beyond captopril. *Toxicon : official journal of the International Society on Toxinology* **2012**, *59*, 516–523, [10.1016/j.toxicon.2011.07.013].
52. Rocha e Silva, M.; Beraldo, W.T.; Rosenfeld, G. Bradykinin, a hypotensive and smooth muscle stimulating factor released from plasma globulin by snake venoms and by trypsin. *The American journal of physiology* **1949**, *156*, 261–273.

53. Ferreira, S.H. A Bradykinin-potentiating factor (BPF) present in the venom of *Bothrops jaracara*. *British journal of pharmacology and chemotherapy* **1965**, *24*, 163–169.
54. Cushman, D.W.; Cheung, H.S.; Sabo, E.F.; Ondetti, M.A. Design of potent competitive inhibitors of angiotensin-converting enzyme. Carboxyalkanoyl and mercaptoalkanoyl amino acids. *Biochemistry* **1977**, *16*, 5484–5491, [10.1021/bi00644a014].
55. Higuchi, S.; Murayama, N.; Saguchi, K.; Ohi, H.; Fujita, Y.; Camargo, A.C.; Ogawa, T.; Deshimaru, M.; Ohno, M. Bradykinin-potentiating peptides and C-type natriuretic peptides from snake venom. *Immunopharmacology* **1999**, *44*, 129–135, [10.1016/S0162-3109(99)00119-8].
56. Wagstaff, S.C.; Favreau, P.; Cheneval, O.; Laing, G.D.; Wilkinson, M.C.; Miller, R.L.; Stöcklin, R.; Harrison, R.A. Molecular characterisation of endogenous snake venom metalloproteinase inhibitors. *Biochemical and biophysical research communications* **2008**, *365*, 650–656, [10.1016/j.bbrc.2007.11.027].
57. Huang, K.F.; Hung, C.C.; Wu, S.H.; Chiou, S.H. Characterization of three endogenous peptide inhibitors for multiple metalloproteinases with fibrinogenolytic activity from the venom of Taiwan habu (*Trimeresurus mucrosquamatus*). *Biochemical and biophysical research communications* **1998**, *248*, 562–568, [10.1006/bbrc.1998.9017].
58. Murakami, T.; Kamikado, N.; Fujimoto, R.; Hamaguchi, K.; Nakamura, H.; Chijiwa, T.; Ohno, M.; Oda-Ueda, N. A [Lys 49]phospholipase A 2 from *Protobothrops flavoviridis* Venom Induces Caspase-Independent Apoptotic Cell Death Accompanied by Rapid Plasma-Membrane Rupture in Human Leukemia Cells. *Bioscience, Biotechnology, and Biochemistry* **2014**, *75*, 864–870, [10.1271/bbb.100783].
59. Sun, L.-K.; Yoshii, Y.; Hyodo, A.; Tsurushima, H.; Saito, A.; Harakuni, T.; Li, Y.-P.; Kariya, K.; Nozaki, M.; Morine, N. Apoptotic effect in the glioma cells induced by specific protein extracted from Okinawa Habu (*Trimeresurus flavoviridis*) venom in relation to oxidative stress. *Toxicology in Vitro* **2003**, *17*, 169–177, [10.1016/S0887-2333(03)00010-9].
60. Oyama, E.; Takahashi, H. Structures and Functions of Snake Venom Metalloproteinases (SVMP) from *Protobothrops* venom Collected in Japan. *Molecules (Basel, Switzerland)* **2017**, *22*, [10.3390/molecules22081305].
61. Petras, D.; Heiss, P.; Harrison, R.A.; Süssmuth, R.D.; Calvete, J.J. Top-down venomics of the East African green mamba, *Dendroaspis angusticeps*, and the black mamba, *Dendroaspis polylepis*, highlight the complexity of their toxin arsenals. *Journal of proteomics* **2016**, *146*, 148–164, [10.1016/j.jprot.2016.06.018].
62. Laemmli, U.K. Cleavage of structural proteins during the assembly of the head of bacteriophage T4. *Nature* **1970**, *227*, 680–685.
63. Muth, T.; Weilnböck, L.; Rapp, E.; Huber, C.G.; Martens, L.; Vaudel, M.; Barsnes, H. DeNovoGUI: an open source graphical user interface for de novo sequencing of tandem mass spectra. *Journal of proteome research* **2014**, *13*, 1143–1146, [10.1021/pr4008078].
64. Calvete, J.J. Next-generation snake venomics: Protein-locus resolution through venom proteome decomplexation. *Expert review of proteomics* **2014**, *11*, 315–329, [10.1586/14789450.2014.900447].
65. Calvete, J.J. Proteomic tools against the neglected pathology of snake bite envenoming. *Expert review of proteomics* **2011**, *8*, 739–758, [10.1586/EPR.11.61].
66. Vizcaíno, J.A.; Deutsch, E.W.; Wang, R.; Csordas, A.; Reisinger, F.; Ríos, D.; Dianes, J.A.; Sun, Z.; Farrah, T.; Bandeira, N.*; et al.* ProteomeXchange provides globally coordinated proteomics data submission and dissemination. *Nature biotechnology* **2014**, *32*, 223–226, [10.1038/nbt.2839].